

Valence quark contributions for the $\gamma^*N \rightarrow N(1440)$ form factors from Light-Front holography

G. Ramalho^a and D. Melnikov^{a,b}

^a*International Institute of Physics, Federal University of Rio Grande do Norte,
Campus Universitário - Lagoa Nova, CP. 1613 Natal Rio Grande do Norte 59078-970, Brazil and*

^b*Institute for Theoretical and Experimental Physics,
B. Chermushkinskaya 25, 117218 Moscow, Russia*

(Dated: March 14, 2017)

The structure of the nucleon and the first radial excitation of the nucleon, the Roper, $N(1440)$, is studied within the formalism of Light-Front holography. The nucleon elastic form factors and $\gamma^*N \rightarrow N(1440)$ transition form factors are calculated under the assumption of the dominance of the valence quark degrees of freedom. Contrary to the previous studies, the bare parameters of the model associated with the valence quark are fixed by the empirical data for large momentum transfer (Q^2) assuming that the corrections to the three-quark picture (meson cloud contributions) are suppressed. The $\gamma^*N \rightarrow N(1440)$ transition form factors are then calculated without any adjustable parameters. Our estimates are compared with results from models based on valence quarks and others. The model compares well with the $\gamma^*N \rightarrow N(1440)$ transition form factor data, suggesting that meson cloud effects are not large, except in the region $Q^2 < 1.5 \text{ GeV}^2$. In particular, the meson cloud contributions for the Pauli form factor are small.

I. INTRODUCTION

Within the nucleon excited states (N^*) the $N(1440)$ resonance, also known as Roper, plays a special role. Contrarily to the $\Delta(1232)$ and other nucleon excitations, the Roper was not identified as a bump in a reaction cross-section but was instead found in the analysis of phase-shifts [1]. Nowadays there is evidence that the Roper should be identified as the first radial excitation of the nucleon quark core, although meson excitations are also important for the internal structure.

Calculations based on valence quark degrees of freedom are consistent with the $\gamma^*N \rightarrow N(1440)$ transition form factors for large Q^2 ($Q^2 > 2 \text{ GeV}^2$) [2–7]. However, estimates based exclusively on quark degrees of freedom fail to describe the small Q^2 data ($Q^2 < 2 \text{ GeV}^2$) [2, 8, 9]. The gap between valence quark models and the data at low Q^2 has been interpreted as the manifestation of the meson cloud effects [3, 4, 7, 10]. When the meson cloud contributions are included in quark models the estimates approach the data [11–16].

Besides, the calculations based on dynamical coupled-channel reaction models, where the baryon excitations are described as baryon-meson states with extended baryon cores [17, 18], corroborates the importance of the meson cloud effects. In those models the mass associated with the Roper bare core is about 1.7 GeV. Only when the meson cloud dressing is considered the Roper mass is reduced to the experimental value [19]. The interpretation of the Roper as a radial excitation of the nucleon combined with a dynamical meson cloud dressing solves the long standing problem of the Roper mass in the con-

text of a quark model [21].

The Roper decay widths into γN , πN and $\pi\pi N$ are large comparative to other N^* decays. Those decay widths are also difficult to explain in the context of a quark model. The meson cloud dressing helps to explain the $N(1440) \rightarrow \gamma N$ width, where the contributions associated with baryon-meson-meson states play an important role [14, 15, 19, 20].

Overall the recent developments in the study of the Roper electromagnetic structure point to the picture of a radial excitation of the nucleon surrounded by a cloud of mesons [10, 15, 19, 22–24]. There is therefore a strong motivation to study the Roper internal structure and to disentangle the effects of the valence quark component from the meson cloud component. In particular, one can use the knowledge of the baryon core structure to infer the contribution due to the meson cloud. This procedure was used in previous works based on different frameworks for the baryon core [3, 4, 7, 10].

In the case of the nucleon the valence quark degrees of freedom produce the dominant effect in the elastic form factors. The meson cloud contribution to the nucleon wave function is estimated to be of the order of a few percent [25–28]. As for the Roper, the meson cloud seems to play a more prominent role. We conclude at the end that the valence quark degrees of freedom provide a very good description of the data, but the meson cloud contribution are important below 1.5 GeV^2 , particularly for the Dirac form factor.

In the present work we propose a new framework to analyze the role of the valence quarks and the meson cloud in the Roper. We use Light-Front holography to estimate the leading order (lowest Fock state) contribution

to the $\gamma^*N \rightarrow N(1440)$ transition form factors. Since the leading order calculation includes only pure valence quark effects in the baryon wave functions (qqq contributions), there is no contribution from the meson cloud. In those conditions the gap between the calculations and the data must be essentially the consequence of the meson cloud effects.

The Light-Front (LF) formalism is particularly appropriate to study hadron systems, ruled by QCD, and to describe the hadronic structure in terms of the constituents [29–31]. The LF wave functions (LFWF) are relativistic and frame independent [30, 32]. The connection between LF quantization of QCD and anti-de-Sitter conformal field theory (AdS/CFT) leads to Light-Front holography [30, 31, 33]. LF holography have been used to study the structure of hadron properties, such as the hadron mass spectrum, parton distribution functions, meson and baryon form factors etc. [8, 30, 31, 33–47]. In particular, the formalism was recently applied to the study of the nucleon [48–54] and Roper [31, 55] electromagnetic structure.

An important advantage of the LF formalism applied to hadronic physics is the systematic expansion of the wave functions into Fock states with different number of constituents [30, 32, 56]. In the case of the baryons the leading order contributions is restricted to the three-valence quark configuration. Although the restriction to the lowest order Fock state (three valence-quark system) may look as a rough simulation of the real world, it may provide an excellent first approximation when the confinement is included in the LFWF, defined at the Light-Front time [25, 33, 36]. In those conditions non-perturbative physics is effectively taken into account by LF holography [30, 36].

Under the assumption that LF holography can describe accurately the large- Q^2 region dominated by valence quark degrees of freedom, we calibrate the free parameters of the model by the available data above a given threshold $Q^2 \geq Q_m^2$ ($Q_m^2 = 1.5\text{--}2.5 \text{ GeV}^2$). This procedure differs from the previous studies where the free parameters, associated with the nucleon anomalous magnetic moments were fixed at $Q^2 = 0$, where the meson cloud contamination is expected to be stronger. Once the free parameters are fixed by the nucleon data, one uses the model to calculate the $\gamma^*N \rightarrow N(1440)$ transition form factors. Since no parameter is adjusted by the Roper data, our calculations are true predictions for the $\gamma^*N \rightarrow N(1440)$ transition form factors.

This article is organized as follows: In Sec. II we discuss LF holography. In the following section (Sec. III), we review the results for the nucleon form factors and fix the parameters by the nucleon data. Our results for the valence quark contribution to the $\gamma^*N \rightarrow N(1440)$ transition form factors and their discussion are presented in Sec. IV. The outlook and conclusions are presented in Sec. V.

II. LIGHT-FRONT HOLOGRAPHY

It is by now well known that string theory or gravity in anti-de-Sitter (AdS) space can provide a description of some lower-dimensional (conformal) gauge theories (CFT) at strong coupling [57–59]. This AdS/CFT correspondence, or holography, can, with certain important restrictions, be applied to QCD-like theories, e.g. [60–62]. It remains an open question, however, whether the *top-down* string theory methods are practical enough to model QCD itself. Instead it proved efficient to apply *bottom-up* approaches to QCD [41, 63, 64]. Such approaches are motivated phenomenologically by the string models, but lack a first-principle justification. Among those, the approach of LF holography is based on a comparison of the results of the LF quantization of QCD [65, 66] with the predictions of holographic (AdS/CFT) models [30, 31, 50, 51, 53].

A. Light-Front QCD vs AdS/CFT

Light-Front quantization provides a powerful tool to study systems ruled by microscopic QCD dynamics. It starts with introducing a special (Light-Front) parametrization of the Hamiltonian, which consequently acts on a Hilbert space of the LFWF spanned by partonic Fock states associated with quarks and gluons [30, 31].

Using LF parametrization one can separate the relative and the overall kinematics of partons obtaining wave functions $\psi_n(\boldsymbol{x}_i, \mathbf{k}_{\perp i})$ where \boldsymbol{x}_i is the fraction of momentum of the parton i , $\mathbf{k}_{\perp i}$ is the transverse momentum and n is the number of components of the Fock state. Functions $\psi_n(\boldsymbol{x}_i, \mathbf{k}_{\perp i})$ define the probability of the given n -parton Fock state. In the massless quark limit, considering the 2D Fourier transform from \mathbf{k}_{\perp} to the transverse impact variable \mathbf{b}_{\perp} , one passes to a wave function defined in the transverse impact space, $\psi_n(\boldsymbol{x}, \mathbf{b}_{\perp})$ [30].

In the semiclassical approximation, when the quark loops are neglected and the quarks are massless, one can replace the dependence on the variables \boldsymbol{x} and \mathbf{b}_{\perp} in ψ_n by dependence on a single parameter $\zeta = \boldsymbol{x}(1 - \boldsymbol{x})|\mathbf{b}_{\perp}|$, except for an overall factor $f(\boldsymbol{x}) = \sqrt{\boldsymbol{x}(1 - \boldsymbol{x})}$ [30, 34, 53]. The variable ζ measures the separation between the active quark and the remaining spectator partons.

The key observation of LF holography is the equivalence of characteristic LFWFs $\psi_n(\boldsymbol{x}, \zeta)$ and wave functions of matter fields in five-dimensional anti-de-Sitter (AdS₅) space, assuming that one identifies ζ with the radial coordinate of AdS₅ [30, 34, 67]. The residual \boldsymbol{x} dependent factor $f(\boldsymbol{x})$ is not relevant in the holographic correspondence, since its effect can be absorbed in the normalization factors in the 5D theory calculation of matrix elements.

The full LFWF is an expansion over n -parton Fock states $|n\rangle$ with coefficients $\psi_n(\boldsymbol{x}, \zeta)$. In the standard terminology those are the states of a given *twist* $\tau \equiv n$. The purpose of this work is to understand the leading twist

contribution ($\tau = 3$), which corresponds to the valence quark approximation to certain QCD processes.

To study the electromagnetic properties of the nucleon excitations we note that a three-quark system ($\tau = 3$), as the nucleon and the nucleon radial excitations can be regarded as two-body systems with an active quark and a spectator cluster with masses (eigenvalues) and wave functions determined by the LF wave equation [30].

B. 5D fermion in AdS space

In the bottom-up holographic approach to QCD the nucleon and the nucleon excitations can be introduced as fermion fields in five-dimensional AdS space [68]. To define this curved space one requires the metric tensor g , which can be conveniently introduced via line element ds^2 in the Poincaré coordinates:

$$ds^2 = \frac{R^2}{z^2} (\eta_{\mu\nu} dx^\mu dx^\nu - dz^2), \quad (2.1)$$

where $\eta_{\mu\nu} = \text{diag}(+, -, -, -)$ is the 4D Minkowski metric tensor and R is a parameter called AdS radius. The latter sets the scale for the space's curvature. AdS₅ radial coordinate z is to be identified with the LF parameter ζ .

From the metric one can define the Dirac operator \hat{D} , which we write as

$$\hat{D} = \frac{i}{2} e_A^M \Gamma^A \left(\overleftrightarrow{\partial}_M + \frac{1}{8} \omega_M^{AB} [\Gamma^A, \Gamma^B] \right). \quad (2.2)$$

Here Γ^A , $A, B = 0, 1, 2, 3, z$ is the standard set of five Dirac gamma matrices and we choose to represent in the chiral basis. Frame e_A^M and spin-connection ω_M^{AB} tensor fields can be computed from the metric tensor. For completeness we summarize the explicit formulas here

$$e_A^M \Gamma^A = \frac{z}{R} (\gamma^\mu, -i\gamma_5), \quad (2.3)$$

$$\omega_M^{AB} = \frac{1}{z} (\eta^{Az} \delta_M^B - \eta^{Bz} \delta_M^A) \quad (2.4)$$

It is also understood that $A \overleftrightarrow{\partial}_M B = A(\partial_M B) - (\partial_M A)B$.

Substantiating the above claim, the kinematic properties of nucleons, *e.g.* the spectrum, can be described by a theory of a massive fermion in AdS₅:

$$S_N = \int d^4x dz \sqrt{-\det g} \bar{\Psi} (\hat{D} - \mu - \Phi) \Psi, \quad (2.5)$$

where μ is the 5D fermion mass to be fixed below.

The function $\Phi(z)$ is an effective scalar potential, whose role is to introduce the complex dynamics of QCD, essentially the confinement. When $\Phi = 0$, the equations of motion of the 5D theory can be cast in the form corresponding to the LF Schrödinger equation in the conformal limit [30]. A phenomenologically compelling choice of the potential is [49, 50]

$$\Phi = \kappa^2 z^2. \quad (2.6)$$

The dimensionful parameter κ breaks conformal symmetry and introduces a mass scale, which determines the meson and baryon spectrum [30, 31, 36]. It can be thus related to Λ_{QCD} . A conventional way to introduce this potential is through the dilaton field background [49, 69]. This procedure makes the connection with top-down AdS/CFT constructions. The corresponding bottom-up case is dubbed the soft-wall model.

In four dimensions the four-component Dirac spinor describes two independent chirality modes. Although five-dimensional Dirac spinor Ψ equally has four components, it will correspond to a nucleon with a specific single choice of chirality. This is a consequence of boundary conditions necessary in the holographic approach [49, 50, 70–72]. In order to preserve CP invariance, the second chirality mode is introduced similarly as Eq. (2.5), but with an opposite sign in front of μ and Φ , *e.g.* [50]. For simplicity of presentation we only review one chirality mode here.

C. Wave equations and wave functions

In order to solve the Dirac equations derived from action (2.5) the fermion field (spin 1/2 and positive parity) Ψ is decomposed into its left- and right- chirality components:

$$\Psi(x, z) = \Psi_L(x, z) + \Psi_R(x, z), \quad (2.7)$$

where $\Psi_{L/R} = \frac{1}{2}(1 \mp \gamma^5)\Psi$. The solution can then be found via separation of variables, assuming a plane wave dependence on the 4D spacetime coordinates

$$\Psi_{L/R}(x, z) = \psi_{L/R}(x) z^2 F_{L/R}(z), \quad (2.8)$$

where left and right Weyl spinors $\psi_{L/R}(x) = \psi_{L/R,P} e^{iP \cdot x}$ satisfy the 4D Dirac equation with mass $M^2 = P^2$. We also pull out the z^2 factor for convenience. In the end, one is left with a pair of coupled equations for scalar *profile* functions $F_{L/R}(z)$:

$$\left[\pm \partial_z + \frac{\mu R + \Phi}{z} \right] F_{L/R}(z) = M F_{R/L}(z). \quad (2.9)$$

The equations must be solved with an appropriate choice of boundary conditions. First, holography requires regularity of the wave function $\Psi(x, z)$ as $z \rightarrow \infty$. For $z \rightarrow 0$ there are two linearly independent solutions $F_{L/R} \sim z^{\mp \mu R}$. In holography one usually chooses to call one of those solutions the source and another one the vev of the operator dual to the bulk (5D) field Ψ – in this case baryon interpolating operator. For the problem in question it only makes sense to choose the vev solution as $F_R \sim z^{\mu R}$ and the source $F_L = 0$. The opposite choice, source $F_R = 0$ and vev $F_L \sim z^{-\mu R}$ leads to a non-physical spectrum. Note that for the opposite chirality case one changes $\mu \rightarrow -\mu$, and the two choices of the $z \rightarrow 0$ boundary conditions are interchanged, with the physical one being $F_R = 0$ and $F_L \sim z^{\mu R}$.

After fixing the boundary conditions it is standard to rewrite system (2.9) as a second order Schrödinger-like differential equation for either F_R , or F_L . Since we are solving the boundary problem, any solution can be expanded over an eigenfunction basis, labeled by an integer n . Equation

$$-\frac{d^2}{dz^2}F_R + \frac{m(m-1)}{z^2}F_R + 2\kappa^2\left(m + \frac{1}{2}\right)F_R + \kappa^4 z^2 F_R = M_n^2 F_R, \quad (2.10)$$

has a set of eigenfunctions $F_{L/R,n}(z)$ expressed in terms of the generalized Laguerre polynomials L_n^α :

$$F_{R,n}(z) \propto z^m e^{-\kappa^2 z^2/2} L_n^{m-1/2}(\kappa^2 z^2). \quad (2.11)$$

The second component F_L can now be calculated using Eqs. (2.9):

$$F_{L,n}(z) \propto z^{m+1} e^{-\kappa^2 z^2/2} L_n^{m+1/2}(\kappa^2 z^2). \quad (2.12)$$

These eigenfunctions correspond to eigenvalues given by

$$M_n^2 = 4\kappa^2 \left(n + m + \frac{1}{2}\right). \quad (2.13)$$

We recall that in the previous expressions $m \equiv \mu R$.

The eigenvalues provide the result for the 4D spectrum of nucleon excitations with radial excitation quantum number n and angular momentum quantum number linear in the parameter m , which we will fix below. The above choice of the potential (2.6) leads to the spectrum consistent with Regge trajectories [30, 31, 41].

Summing up, the full solution for the 4D positive chirality mode reads

$$\Psi_n^+(x, z) = z^2 \begin{pmatrix} F_{L,n}(z) \chi_n(x) \\ F_{R,n}(z) \chi_n(x) \end{pmatrix}, \quad (2.14)$$

where $\chi_n(x)$ are two component spinors related with the Weyl spinors: $\psi_L^\dagger(x) = (\chi_n^\dagger(x), 0)$ and $\psi_R^\dagger(x) = (0, \chi_n^\dagger(x))$. The negative chirality modes is obtained via an appropriate change of signs and exchange of the solutions for $F_{L/R}$ [50, 55]:

$$\Psi_n^-(x, z) = z^2 \begin{pmatrix} F_{R,n}(z) \chi_n(x) \\ -F_{L,n}(z) \chi_n(x) \end{pmatrix}. \quad (2.15)$$

Using the component associated with the index n we can write the fermion fields with positive and negative parities as

$$\Psi^\pm(x, z) = \frac{1}{\sqrt{2}} \sum_n \Psi_n^\pm(x, z). \quad (2.16)$$

D. Interactions

In hadron physics, information on the structure of nucleon resonances is contained in the matrix elements

of interaction currents between the initial and final hadrons, including the nucleon and the nucleon excitations (baryons). In holography, 4D operators of conserved currents J_μ are described by massless gauge fields V_M in AdS_5 space. Interacting bulk baryon fields Ψ couple to the gauge fields, which is a dual holographic description of the coupling of baryons to conserved currents. Matrix elements of the currents, can be computed from the interaction terms, which are, schematically, overlaps of the bulk fields with the source gauge field [73]:

$$S_{\text{int}} = \int d^4x dz \sqrt{-\det g} \bar{\Psi}(x, z) \hat{\mathcal{V}}(x, z) \Psi(x, z). \quad (2.17)$$

Here $\hat{\mathcal{V}}$ encodes a coupling of field V_M to fermions. We consider in particular the decomposition

$$\hat{\mathcal{V}}(x, z) = \hat{\mathcal{V}}_0(x, z) + \hat{\mathcal{V}}_1(x, z) + \hat{\mathcal{V}}_2(x, z), \quad (2.18)$$

as discussed next. For simplicity, we only present the interaction for positive chirality. For the opposite chirality case one has to adjust the signs in the above expression to preserve the CP invariance [50].

The term $\hat{\mathcal{V}}_0(x, z)$ is representing the minimal Dirac coupling given by [49]

$$\hat{\mathcal{V}}_0(x, z) = \hat{Q} \Gamma^M V_M(x, z), \quad (2.19)$$

where V_M could be either the abelian dual of the electromagnetic current, or the non-abelian isovector current. Following the parametrization of [50, 55] $\hat{Q} = e_N = \frac{1}{2}(1 + \tau_3)$, the nucleon charge ($N = p, n$), for the elastic electromagnetic transitions, and $\hat{Q} = \tau_3$ for the transition between the nucleon and higher mass $J^P = \frac{1}{2}^+$ resonances (τ_3 is the Pauli isospin operator). This *minimal* coupling only yields the Dirac form factor.

To produce the Pauli form factor more input from the holographic side is necessary. Abidin and Carlson [49] proposed to consider a non-minimal extension of the coupling $\hat{\mathcal{V}}_0$, adding a term

$$\hat{\mathcal{V}}_1(x, z) = \frac{i}{4} \eta_N [\Gamma^M, \Gamma^N] V_{MN}(x, z), \quad (2.20)$$

where $V_{MN} = \partial_M V_N - \partial_N V_M + [V_M, V_N]$ and one can consider different couplings η_S and η_V for the isoscalar and isovector parts respectively [$\eta_N = \frac{1}{2}(\eta_S + \eta_V \tau_3)$]. As one may expect from its Lorentz structure, this term yields the Pauli form factors, as well as a correction to the Dirac form factors. Moreover, since the non-minimal term contains derivatives of the field V_M and extra powers of z , the Pauli form factor turns out to be subleading with respect to the Dirac form factor at large momentum transfer, as expected, while the correction to the Dirac form factor is of the same order. The effect of the term \mathcal{V}_1 on the nucleon form factors is studied in Refs. [31, 49–52, 55]. We provide additional details in what follows.

More non-minimal couplings can be considered. In Refs. [50, 55] the following non-minimal (isovector) term was suggested

$$\hat{\mathcal{V}}_2(x, z) = g_V \tau_3 \Gamma^M \gamma^5 V_M(x, z). \quad (2.21)$$

where g_V is a coupling constant. This coupling is consistent with gauge invariance and discrete symmetries, that can be added to the 5D action to improve the fitting of experimental data [50].

One first observation about this term is that it naively breaks CP in 4D. However, this is not the case, since 5D fermion Ψ describes only one 4D chirality. Adding a similar interaction term for the opposite chirality, with the opposite sign of coupling, ensures 4D CP invariance.

A more serious issue is that Eq. (2.21) breaks 5D covariance. Adding such term requires an implicit background 5D vector field. Such background fields are more common in the higher-dimensional top-down holographic models with flux compactifications. Here we assume that such a flux compactification exists and we assess its effect on the observable form factors. We further comment on the general structure of the term (2.17) in Ref. [74].

In order to calculate transition matrix elements of the currents using Eq. (2.17) one needs to specify the 5D gauge field $V_M(x, z)$. Similarly to fermions, a bosonic gauge field dual to the isovector or isoscalar current is introduced by a 5D Lagrangian. Specifically, one needs to solve equations following from the action

$$S_J = - \int d^4x dz \sqrt{-\det g} \frac{e^{-\Phi}}{4} \text{Tr} V_{MN} V^{MN}, \quad (2.22)$$

subject to appropriate boundary conditions. These boundary conditions differ from the boundary conditions for the fields associated with the nucleon and the nucleon excitations characterized by the quantum numbers n and m , since they have to be of the *source* type at $z = 0$ (the leading solution as opposed to the subleading vev-type). The regularity condition requires V_M to vanish for $z \rightarrow \infty$.

In what follows we will be interested in the abelian electromagnetic current, so the non-abelian details of this discussion can be omitted. Altogether, the solution can be cast in the form [50, 55, 75]

$$V_\mu(x, z) = \int \frac{d^4q}{(2\pi)^4} e^{-iq \cdot x} \epsilon_\mu(q) V(-q^2, z), \quad (2.23)$$

where ϵ_μ is the photon polarization vector, and

$$V(Q^2, z) = \kappa^2 z^2 \int_0^1 \frac{d\kappa}{(1-\kappa)^2} x^{\frac{Q^2}{4\kappa^2}} e^{-\frac{\kappa^2 z^2 \kappa}{1-\kappa}}, \quad (2.24)$$

with $Q^2 = -q^2$. In the limit $z \rightarrow 0$, one has $V(Q^2, 0) = 1$.

Substituting Eqs. (2.23) and (2.24) together with the modes (2.14) and (2.15) into the interaction Lagrangian (2.17) yields matrix elements of the current up to some normalization terms, from which form factors are read off directly. We present the results in Sec. III for the nucleon and in Sec. IV for the Roper.

E. Mass spectrum and more

In this section we specify the details of the holographic model and relating it to the observable spectrum of the

nucleon radial excitations and the ρ mesons.

First, the nucleon (Ψ_{N0}) and the Roper (Ψ_{N1}) are the states with radial quantum numbers $n = 0, 1$ and angular momentum $L = 0$. Any of these states must be regarded as a superposition of the given twist (number of partons) Fock states, so we assume that the 5D mass μ is encoding both the angular momentum L and the twist τ , $\mu R = m(L, \tau)$.

A way to fix the relation for $L = 0$ is to analyze the large Q^2 scaling of $F_{L/R,n}(z)$ and consequently the form factors. As discussed later, the choice $m = \tau - 3/2$ yields the correct falloff estimated by perturbative QCD (pQCD) [76]. Consequently, the spectrum (2.13) takes the following form [30, 31, 55],

$$M_{Nn} = 2\kappa\sqrt{n + \tau - 1}. \quad (2.25)$$

Thus, holography provides an estimate for the spectrum of the nucleon radial excitations in terms of a single scale parameter κ . Similarly, one obtains the spectrum of mesons and baryons with different angular momenta and parity [30, 31, 36].

The ρ meson (mass m_ρ) is a traditional reference for the hadron states. In LF holography we can write $m_\rho = 2\kappa$. The nucleon mass, for example, approximately satisfies $M_N = \sqrt{2}m_\rho$. If we assume that the nucleon mass is primarily composed of the leading twist $\tau = 3$ contribution, $M_N = 2\sqrt{2}\kappa$, then the phenomenological value of κ is fixed at

$$\kappa = \frac{m_\rho}{2} \sim \Lambda_{\text{QCD}}. \quad (2.26)$$

The leading twist estimate of the masses of nucleon radial excitations is now given by $M_{Nn} = 2\kappa\sqrt{n + 2}$, $n = 0, 1, 2, \dots$. This yields $M_R = M_{N1} = 2\sqrt{3}\kappa$ for the Roper mass in leading twist approximation ($\tau = 3$).

It is worth mentioning that the LF estimate of the Roper mass, $M_R \simeq \sqrt{3}m_\rho$, is not so accurate as for the nucleon and the ρ meson. This is consistent with a general expectation that leading twist approximation is not so accurate for baryons as it is for mesons. In particular for the Roper, there are indications that the baryon-meson-meson corrections of the twist order $\tau = 7$ are important [19, 20]. In the next subsection we collect further comments on the spectrum and other issues of LF holography.

The spectrum of the hadrons, as predicted by LF holographic approach has further issues. A similar approach to mesons yields similar Regge-behaved spectra as the one given by Eq. (2.25). For the ρ meson family one gets $m_{\rho n} = 2\kappa\sqrt{n + 1}$ for $n = 0, 1, 2, \dots$ [41, 44, 75]. Brodsky and Teramond argue, however, that those twist-2 mass poles should be shifted to their physical values, suggesting that $m_{\rho n} = 2\kappa\sqrt{2n + 1}$ [30, 36, 54]. These formula gives a very good agreement with the vector meson masses for $\kappa \simeq 0.385$ GeV [30, 36], as in Eq. (2.26), provided that $m_\rho \simeq 770$ MeV. Similar values were used in Refs. [50, 55].

F. Comments on interpolating operators in LF holographic approach

The scaling dimension Δ is defined by the behavior of the wave function in the limit $z \rightarrow 0$: $\Psi(x, z) \sim z^\Delta$ [33, 49]. The holographic approach relates the 5D mass parameter m with the scaling dimension Δ of the hadron interpolating operator. For example, for the vector field this relation is

$$\Delta = 2 + \sqrt{m^2 + 1}. \quad (2.27)$$

For the massless vector field V_M above, this infers $\Delta = 3$, the correct scaling dimension of a current operator [33]. For fermions however the relation is

$$\Delta = 2 + |m|. \quad (2.28)$$

In the leading twist this yields $\Delta = 7/2$ for the nucleon/Roper interpolating operator, in contrast to the scaling dimension $\Delta_{\mathcal{O}} = 9/2$ of the operator $\mathcal{O} = qq\bar{q}$, composed of three quark fields. This discrepancy is even more pronounced if one applies the identification $m(\tau, L)$ used in Ref. [30]. Indeed, comparing Eqs. (2.11) and (2.13) with Eqs. (5.34) and (5.38) of Ref. [30] one ends up with the relation $m = \nu + 1/2$, which implies $\Delta = 5/2$.

In QCD the (anomalous) scaling dimensions of the interpolating operators are not well-defined, because of the logarithmic running of the gauge coupling. In a putative conformal theory, which would approximate the slow running of the coupling, the anomalous scaling dimensions would exist and correspond to a dual gravity theory of the type studied here. In particular, the massless vector field of a gravity dual would correspond to $\Delta = 3$ conserved symmetry current. In the meantime we have to accept that the correct choice of the operator dimension leads to unpleasant effects like incorrect scaling of the form factors for very large Q^2 .

One can argue, in principle, that predictions of holographic models are generally valid in the strongly coupled regime of a theory, thus the pQCD prediction should not be compared with the outcome of the holographic analysis. We believe, however, that this argument does not quite apply to the scaling of the form factors, since the pQCD prediction is rather based on the assumption of a particular partonic structure of the hadron, which is not exactly the full perturbative quark picture [76].

We hope that some more advanced holographic model can resolve the issues mentioned above. In particular, top-down models, as more complex ones, naturally share more intricate details with QCD. A prototypical example would be (the glueball sector of) the Klebanov-Strassler theory [61, 77]. Albeit supersymmetric, this theory encodes a logarithmically running gauge coupling, thus, extracting dimensions of the operators in this theory requires removing the logarithmic scale dependence (*e.g.* [78–80]). Moreover, in this theory, the states with the same quantum numbers tend to mix with

each other. Therefore the mass eigenstates are superpositions of states with different twist. Mixing has effect of changing the resulting spectrum as well as shifting the values of the dimensions [79–83].

III. NUCLEON ELECTROMAGNETIC FORM FACTORS

The transition current J^μ between two nucleon states (elastic transition) can be expressed, omitting the asymptotic spin states (spinors) and the electric charge e , as [8, 26]

$$J^\mu = F_{1N}(Q^2)\gamma^\mu + F_{2N}(Q^2)\frac{i\sigma^{\mu\nu}q_\nu}{2M}, \quad (3.1)$$

where F_{iN} ($i = 1, 2$) define, respectively, the Dirac and Pauli form factors of the proton ($N = p$) and neutron ($N = n$). In the LF formalism, the two form factors appear in a spin-nonflip (F_{1N}) and a spin-flip (F_{2N}) transitions [56, 84].

The calculation of the overlaps (2.17) in the holographic model with the interaction (2.18), where one replaces Ψ and $\bar{\Psi}$ by the appropriate initial and final nucleon state modes, in this case the nucleon modes Ψ_{N0} . The leading twist case ($\tau = 3$), the Dirac form factor is determined by the functions $F_{L,0}^2$ and $F_{R,0}^2$, and the Pauli form factor is determined by overlap of the $F_{L,0}$ and $F_{R,0}$ components [50, 55]. The final expressions for the form factors are then [50]:

$$F_{1N} = e_N \frac{a+6}{(a+1)(a+2)(a+3)} + g_V \delta_N \frac{a}{(a+1)(a+2)(a+3)} + \eta_N \frac{2a(2a-1)}{(a+1)(a+2)(a+3)(a+4)}, \quad (3.2)$$

$$F_{2N} = \eta_N \frac{M_N}{2\sqrt{2}\kappa} \frac{48}{(a+1)(a+2)(a+3)}, \quad (3.3)$$

where $a = \frac{Q^2}{4\kappa^2}$ and κ is the holographic scale discussed in the previous section. In Eqs. (3.2)-(3.3), $\delta_N = \pm 1$ ($\delta_p = 1$, $\delta_n = -1$) and η_N take different values for proton and neutron. In Eq. (3.3) we can replace $\frac{M_N}{2\sqrt{2}\kappa}$ by unity, if $2\sqrt{2}\kappa$ is a good approximation for the nucleon mass.

In an exact $SU(2)$ -flavor model one has $\eta_n = -\eta_p$. These parameters can be determined by the proton and neutron bare anomalous magnetic moment κ_p^b and κ_n^b (we use the upper index b to indicate the bare values). In a model with no meson cloud one can write $F_{2p}(0) \equiv \kappa_p = 8\eta_p$ and $F_{2n}(0) \equiv \kappa_n = 8\eta_n$, assuming $M_N = 2\sqrt{2}\kappa$.

The holographic results (3.2)-(3.3) yield the correct perturbative QCD behavior for the nucleon electromagnetic form factors: $F_{1N} \propto 1/Q^4$ and $F_{2N} \propto 1/Q^6$, as consequence of $m = 3/2$. For a more detailed discussion see Refs. [49, 50, 55].

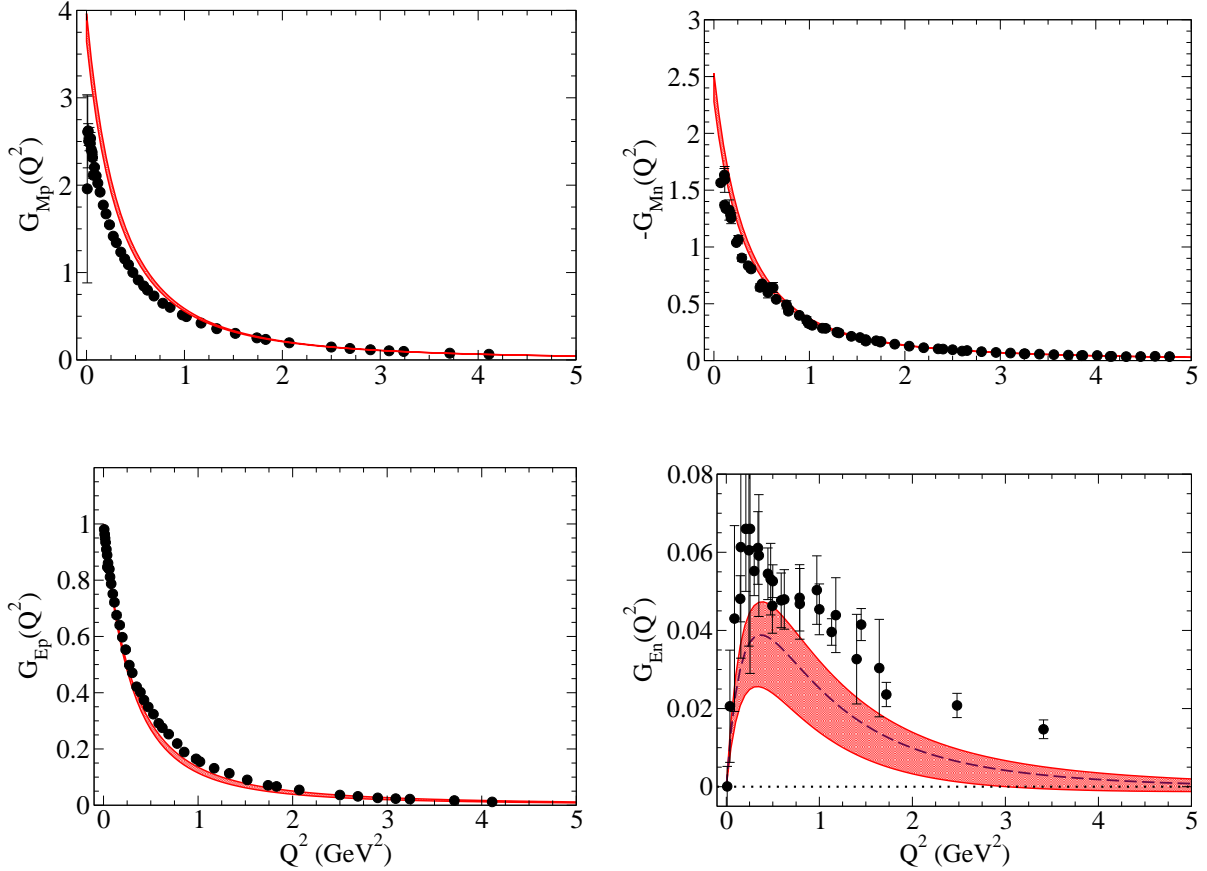


FIG. 1: Proton and neutron electric and magnetic form factors for the parametrization from Table I. In the case of G_{En} the dashed-line corresponds to the parametrization with $Q^2 \geq 2.0$ GeV². Data from Refs. [85–87].

As previously discussed the non-minimal couplings η_N and g_V are included phenomenologically. As can be seen from Eqs. (3.2)-(3.3), the minimal coupling only produces the Dirac form factor. The non-minimal couplings generate a non-zero F_{2N} and adds an extra contribution to the Dirac form factor (proportional to η_N) [37]. Relations of the type (3.2)-(3.3) were derived for the first time in Ref. [49] for the case $g_V = 0$.

To determine the values of g_V and η_N we performed a fit to the data $Q^2 \geq Q_m^2$ where Q_m^2 is the threshold of the data included in the fit. We considered the cases $Q_m^2 = 1.5, 2.0$ and 2.5 GeV², since the meson cloud effects are in principle suppressed for large Q^2 , but we do not know a priori the threshold of the suppression. We use the data from Refs. [85–87]. Check Refs. [27, 28] for a detailed description of the database.

From the fits, we conclude that the results for the neutron electric form factor G_{En} are very sensitive to the value of Q_m^2 . If the low Q^2 is included in the fit ($Q_m^2 < 1.0$ GeV²) the best fit favors a negative G_{En} for low Q^2 , in conflict with the measured data. This result is very pertinent, because it is known that meson cloud effects, in particular the pion cloud, is very important for the description of the G_{En} at low Q^2 . Since the pion cloud

contributions are not included in the parametrization of Eqs. (3.2)-(3.3), it is not surprising to see that the fit with $Q_m^2 = 1.5$ GeV² fails to describe the G_{En} data. It can be surprising, however, to note that the best description of the nucleon data occurs for $Q^2 > 1.5$ GeV² in the fits with $Q_m^2 = 2.0$ and 2.5 GeV², when only a few data points for G_{En} are considered. One then concludes that the shape of G_{En} is determined by the form factors G_{Ep} , G_{Mp} and G_{Mn} . This result shows the consistence of the fitting procedure.

The parameters obtained for the fits with $Q_m^2 = 1.5, 2.0$ and 2.5 GeV² are presented in Table I. We can conclude that the parameters are sensitive to the data included in the fit. In particular, g_V depends strongly of the threshold Q_m^2 .

The results obtained for the nucleon electric ($G_{EN} = F_{1N} - \frac{Q^2}{4M_N^2} F_{2N}$) and magnetic ($G_{MN} = F_{1N} + F_{2N}$) form factors using the parameters from Table I are presented in Fig. 1. In the figure, we include a band to represent the interval between the model with $Q_m^2 = 1.5$ GeV² and 2.5 GeV². In the calculations we used $\kappa = 0.385$ GeV, in order to have a good description of the ρ mesons and nucleon masses.

$Q_m^2 (\text{GeV}^2)$	g_V	η_p	η_n
1.5	1.571	0.378	-0.326
2.0	1.370	0.410	-0.345
2.5	1.275	0.424	-0.361

TABLE I: Parameters g_V , η_p and η_n obtained by the fit of the nucleon form factor data with $Q^2 \geq Q_m^2$.

In general the estimates from different parametrizations are very close, except, for the neutron electric form factor. The function G_{En} is in fact very sensitive to the parameters g_V , η_p and η_n . In the graph of G_{En} the lower limit corresponds to $Q_m^2 = 1.5 \text{ GeV}^2$ and the upper limit to the case $Q_m^2 = 2.5 \text{ GeV}^2$. The intermediate case ($Q_m^2 = 2.0 \text{ GeV}^2$) is included in order to emphasize the strong dependence of G_{En} with the threshold Q_m^2 used in the fit, and it is represented by the dashed-line.

Concerning the remaining form factors, one can notice an overestimation of the low Q^2 data ($Q^2 < 1 \text{ GeV}^2$) for G_{Mp} and $-G_{Mn}$. These results may be interpreted as the manifestation of the pion cloud effects, not included in the formalism associated with Eqs. (3.2)-(3.3).

In the past [37, 50, 55] the parameters η_N and g_V have been fixed by the static properties of the nucleon, such as the anomalous magnetic moments and the nucleon electric charge radius. Since those observables depend on the meson cloud, we choose in this work to fix the parameters in a region where the meson cloud is significantly reduced, in order to obtain a more accurate estimate of the bare parameters.

In the recent work the Brodsky-Teramond model for the nucleon [54] was improved with the inclusion of the explicit pion cloud contributions ($q\bar{q}$ states) with a few adjustable parameters. It was shown that, indeed, the inclusion of the pion cloud contribution ($\tau = 5$) is fundamental for an accurate description of G_{En} .

In order to understand the role of the valence quark degrees of freedom we restrict the present study to the the leading twist contribution ($\tau = 3$). Once fixed the parameters of the model (bare parameters) one can use those parameters to calculate the valence quark contributions for the $\gamma^*N \rightarrow N(1440)$ transition form factors.

IV. $\gamma^*N \rightarrow N(1440)$ FORM FACTORS

We consider now the $\gamma^*N \rightarrow N(1440)$ transition form factors. Again omitting the spinors of the nucleon and the Roper (and the electric charge e), the transition current J^μ can be expressed as [3]

$$J^\mu = F_{1N}^*(Q^2) \left(\gamma^\mu - \frac{\not{q} q^\mu}{q^2} \right) + F_{2N}^*(Q^2) \frac{i\sigma^{\mu\nu} q_\nu}{M + M_R}, \quad (4.1)$$

where F_{1N}^* and F_{2N}^* ($N = p, n$) are the Dirac and Pauli transition form factors, respectively.

Using the holographic wave functions for the nucleon and the Roper combined with the interaction (2.18), one concludes that the Dirac and Pauli form factors associated with the $\gamma^*N \rightarrow N(1440)$ in leading twist [55] are

$$F_{1N}^* = \delta_N \frac{a(\sqrt{2}a + c_1)}{(a+1)(a+2)(a+3)(a+4)} + g_V \delta_N \frac{a(\sqrt{2}a + c_2)}{(a+1)(a+2)(a+3)(a+4)} + \eta_N \frac{2a(2\sqrt{2}a^2 - c_3a + c_4)}{(a+1)(a+2)(a+3)(a+4)(a+5)}, \quad (4.2)$$

$$F_{2N}^* = \eta_N \left(\frac{M_R + M_N}{M_R} \right)^2 \frac{M_R}{2\sqrt{3}\kappa} \times \frac{6\sqrt{3}(c_5a - 4)}{(a+1)(a+2)(a+3)(a+4)}, \quad (4.3)$$

where $c_1 = 4\sqrt{2} + 3\sqrt{3}$, $c_2 = 4\sqrt{2} - 3\sqrt{3}$, $c_3 = 9(\sqrt{3} - \sqrt{2})$, $c_4 = 3\sqrt{3} - 5\sqrt{2}$ and $c_5 = 2 + \sqrt{6}$.

In Eq. (4.3) we can replace $\frac{M_R}{2\sqrt{3}\kappa}$ by unity if $2\sqrt{3}\kappa$ is a good approximation to the Roper mass. In comparison with Ref. [55] we include an extra factor $\frac{M_R + M_N}{M_R}$ in order to be consistent with the more usual definition of the transition form factors (4.1).

The results for the nucleon to Roper transition form factors associated with the parameters g_V , η_p and η_n discussed previously (Table I), are presented in Fig. 2, for the proton target ($N = p$). As for the nucleon we use $\kappa = 0.385 \text{ GeV}$. The data presented here are those from CLAS/Jefferson Lab for single pion production [88] and double pion production [89], and it is collected in the database [90]. We do not discuss the results for the neutron target ($N = n$) because they are restricted to the photon point.

In Fig. 2, we can see that, contrary to the nucleon case, the results are almost insensitive to the variation of parameters, therefore we consider only the upper and lower cases ($Q_m^2 = 1.5$ and 2.5 GeV^2), delimited by the band. In the figure one can see that the holographic approach based on Eqs. (4.2)-(4.3) in the leading twist approximation gives a very good description of the large Q^2 data ($Q^2 > 1.8 \text{ GeV}^2$) in the range $g_V = 1.28, \dots, 1.57$, $\eta_p = 0.38, \dots, 0.42$ and $\eta_n = -(0.36, \dots, 0.32)$.

In the above holographic approach one obtains a clear estimate of the valence quark contributions based on framework that includes only one pre-defined parameter: the mass scale κ . Since the coefficients g_V , η_p , η_n are determined by the nucleon form factors, one can consider this estimate of the valence quark contributions for the nucleon to Roper form factors as a parameter-free prediction.

The present results for F_{1p}^* and F_{2p}^* are consistent with estimates of the form factors based on different frameworks, such as the results of Refs. [2-4, 7, 10]. In particular, the present model and the results of the covariant

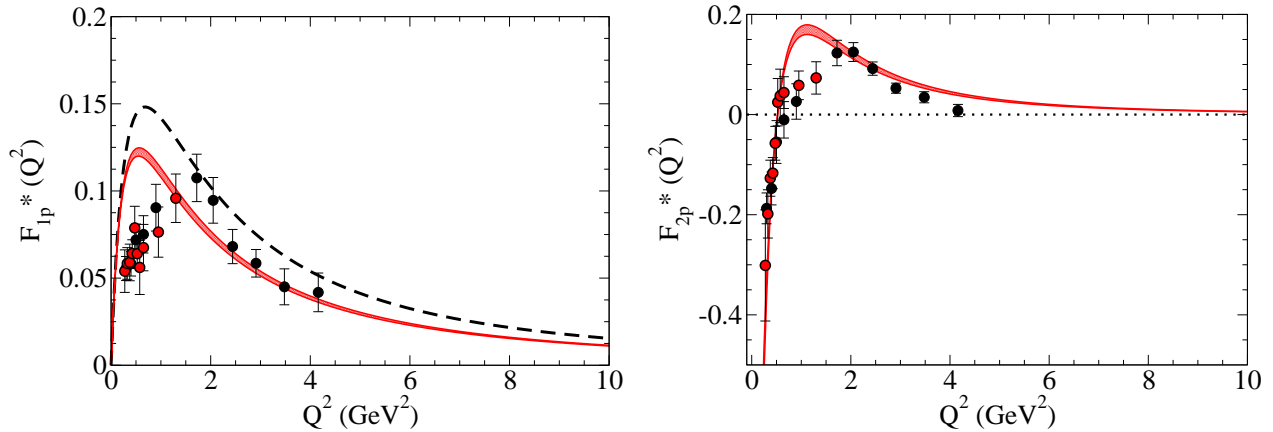


FIG. 2: $\gamma^* N \rightarrow N(1440)$ transition form factors F_{1p}^* and F_{2p}^* . The dashed-line is the result from the Light-Front holographic model from Ref. [31]. Black dots from Ref. [88]; red dots from Ref. [89].

quark model from Refs. [3, 4, 26] are very close for $Q^2 > 5$ GeV^2 .

The original holographic calculation of the nucleon to Roper transition form factors was done in Ref. [55]. In that work higher Fock states (twist 4 and 5 contributions) were also taken into account. However the effective contribution of the higher Fock states was determined by the equation for the Roper mass, and not by the physics associated with the form factors (dominance of the leading twist contributions for large Q^2). In addition, the overlap between the nucleon and Roper states was determined in Ref. [55] using coefficients adjusted to the form factor data.

In the present work we rather prefer to concentrate on deriving a clean estimate of the valence quark contribution using an alternative method of fixing the parameters of the model, instead of trying to estimate the quark-antiquark and gluon contributions using LF holography. Since we do not consider higher twist contributions, the overlap between the states is just the result of the overlap between the valence quark states of both baryons with no unknown coefficients.

Although we conclude that the leading twist calculation is a good approximation for the form factors, one still notes that it may not be sufficient for a satisfactory estimate for the mass of the Roper. Different estimates of the mass suggest, in fact, that higher Fock states are crucial for the explanation of the experimental value [19–21].

In Fig. 2, we also present the estimate of the LF holographic model from Teramond and Brodsky for F_{1p}^* [31]. In their formulation, the Dirac form factor is expressed by an analytic function dependent on the ρ meson masses [31, 36]. The closeness between results is a consequence of the use of the holographic masses instead of the physical masses. We note at this point, that, the relations (4.2)-(4.3) are also analytic parametrization of the Roper form factors, since the form factors are expressed in terms

of functions of $a = \frac{Q^2}{m_\rho^2}$, using $m_\rho^2 = 4\kappa^2$. We leave however the comparison between analytic parametrization of the Roper form factors to a separated work [91].

In the graph for F_{1p}^* one can notice a deviation between our estimate and the data for $Q^2 < 1$ GeV^2 . This result can be interpreted as the consequence of the meson cloud contributions not included in our leading twist analysis. Similar results were obtained in independent works [2, 3, 7]. Sizable contributions of the meson cloud effects were found in Refs. [15, 16].

As for the results for F_{2p}^* , one can note that the parametrization based on the LF holography gives negative values for small Q^2 , and are close to the data. In particular we estimate the change of sign in F_{2p}^* for $Q^2 \approx 0.5$ GeV^2 . The results for F_{2p}^* suggest that contrarily to the form factor F_{1p}^* , where the meson cloud are sizable, for F_{2p}^* the meson cloud contribution are very small at low Q^2 . To the best of our knowledge, it is the first time that this fact was observed in the context of a quark model. There is, nevertheless, a discrepancy between the model and the data in the region between 0.9 and 1.5 GeV^2 .

Concerning the F_{2p}^* data, one can note that in the region 0.9–1.5 GeV^2 there are only two datapoints associated the two pion electroproduction CLAS data [89]. It is important to check if the new data associated with the one pion production confirms the trend from Ref. [89]. At the moment one can conclude that the holographic model gives a very good description of the F_{2p}^* data except for three data points in the range 0.9–1.5 GeV^2 (underestimation of the data in about 60%).

Discussion

Summarizing the results presented here for the nucleon and Roper form factors, one can conclude that the leading twist approximation provides a very good estimate for

both nucleon and Roper form factors. This result is consistent with the LF formalism, because in the Drell-Yan-West frame the contributions from higher Fock states are small [25, 30, 33]. It is expected however that the meson cloud effects provide significant contributions to the $\gamma^*N \rightarrow N^*$ transition form factors for some nucleon excitations N^* for small Q^2 [8, 92–100].

In the present work, the meson cloud effect is observed in particular for the form factors of the Roper: F_{1p}^* , and in the region 0.9–1.5 GeV² for F_{2p}^* . Those meson cloud corrections come from higher twist contributions to the Light-Front wave functions. For higher mass resonances it is expected that higher twist corrections also give important contributions to the transition form factors at low Q^2 . In that case LF holography can be used to estimate mainly the contribution of the quark core. Although the estimate for low Q^2 may appear rough, since the calculation is based on massless quarks (and the physical quarks have mass), for large Q^2 the estimate is expected to be accurate due to the dominance of the valence quark degrees of freedom.

In the future one can use holography to estimate transition form factors in the leading twist approximation for other N^* states. Those estimates are expected to be accurate at large Q^2 , since they are based on valence quark degrees of freedom. At low Q^2 LF holography may fail in leading twist, since the framework provides only the valence quark contributions to the form factors. That information can be, however, very useful to understand the role of the meson cloud contributions. On one hand, we can use the comparison with the data to estimate the effect of the meson cloud contribution. On the other hand, estimates of the bare core can also be used as input to dynamical coupled-channel reaction models in the parametrization of baryon bare core [17–19].

It is worth mentioning that some authors interpret the Roper as a dynamically-generated baryon-meson resonance, without an explicit reference to three-quark systems, except for the nucleon and the $\Delta(1232)$ [101–104]. As far as we know, there are no calculations of $\gamma^*N \rightarrow N(1440)$ transition form factors for intermediate and large Q^2 , based on dynamically-generated resonance models for the Roper. Future lattice QCD simulations can help to understand the role of the baryon-meson contribution for the transition form factors at low Q^2 [103, 104].

V. OUTLOOK AND CONCLUSIONS

In the present work we apply the LF holography in the soft-wall approximation to the study of the electromagnetic structure of the nucleon and nucleon excitations. More specifically we study the nucleon and $\gamma^*N \rightarrow N(1440)$ transition form factors in the leading twist approximation.

Since in the leading twist approximation the transition

form factors are determined by the valence quark degrees of freedom, in the present approach we estimate the contribution of valence quarks to the electromagnetic form factors. The Light-Front wave functions are determined by an appropriate choice of boundary conditions in the 5D space and by the expected pQCD falloff for the Dirac and Pauli form factors (bottom-up approach to QCD).

The Light-Front holography in the soft-wall version was used previously in the study of the nucleon elastic form factors, in leading twist and higher orders. However, since in those works the couplings are adjusted to the dressed couplings (empirical anomalous magnetic moments) they may describe well the low Q^2 data, but fail in the description of the large- Q^2 data. In the present work we fix the free parameters of the model associated with the bare couplings using the large Q^2 data for the nucleon, where the effect of the meson cloud contributions is significantly reduced.

Our expressions for the electromagnetic form factors depend only of the holographic mass scale κ and of three bare couplings: g_V , η_p and η_n . Once determined the bare couplings by the nucleon data, the model is used to predict the $\gamma^*N \rightarrow N(1440)$ transition form factors.

Our results for the $\gamma^*N \rightarrow N(1440)$ transition form factors compare well with the empirical data. For the Dirac form factor, the deviation observed for $Q^2 < 1.0$ GeV² is compatible with the interpretation that meson cloud contributions are important in that region. As for the Pauli form factor, our estimate is very close to the data, both at low and at large Q^2 , except for 3 datapoints in the range 0.9–1.5 GeV². The result at low Q^2 , suggests that the meson cloud contributions for F_{2p}^* are small. As far as we know this is the first time that this effect is observed.

The method used in the present work for the Roper can in the future be extended for higher mass nucleon excitations. The use of the Light-Front holography in leading twist provides then a natural method to estimate the valence quark contributions for the transition form factors. The effect of the meson cloud can then be estimated from the comparison with the experimental data.

Theoretical estimates of the bare core contributions are very important for the study of the baryon-meson reactions and nucleon electroproduction reactions. The results from Light-Front holography may be used as input to dynamical coupled-channel reaction models in the theoretical study of those reactions.

Acknowledgments

G. R. thanks Valery Lyubovitskij for useful clarifications about the calculation of the transition form factors. This work was supported by the Universidade Federal do Rio Grande do Norte/Ministério da Educação (UFRN/MEC). The work of D. M. was also partially supported by the RFBR grant 16-01-00291.

-
- [1] L. D. Roper, Phys. Rev. Lett. **12**, 340 (1964).
- [2] I. G. Aznauryan, Phys. Rev. C **76**, 025212 (2007) [nucl-th/0701012].
- [3] G. Ramalho and K. Tsushima, Phys. Rev. D **81**, 074020 (2010) [arXiv:1002.3386 [hep-ph]].
- [4] G. Ramalho and K. Tsushima, Phys. Rev. D **89**, 073010 (2014) [arXiv:1402.3234 [hep-ph]].
- [5] G. Ramalho and K. Tsushima, AIP Conf. Proc. **1374**, 353 (2011) [arXiv:1010.2765 [hep-ph]].
- [6] E. Santopinto and M. M. Giannini, Phys. Rev. C **86**, 065202 (2012) [arXiv:1506.01207 [nucl-th]].
- [7] J. Segovia, B. El-Bennich, E. Rojas, I. C. Cloet, C. D. Roberts, S. S. Xu and H. S. Zong, Phys. Rev. Lett. **115**, 171801 (2015) [arXiv:1504.04386 [nucl-th]].
- [8] I. G. Aznauryan *et al.*, Int. J. Mod. Phys. E **22**, 1330015 (2013) [arXiv:1212.4891 [nucl-th]].
- [9] I. G. Aznauryan and V. D. Burkert, Prog. Part. Nucl. Phys. **67**, 1 (2012) [arXiv:1109.1720 [hep-ph]].
- [10] I. G. Aznauryan and V. D. Burkert, Phys. Rev. C **85**, 055202 (2012) [arXiv:1201.5759 [hep-ph]].
- [11] F. Cano and P. Gonzalez, Phys. Lett. B **431**, 270 (1998) [arXiv:nucl-th/9804071].
- [12] L. Tiator, D. Drechsel, S. Kamalov, M. M. Giannini, E. Santopinto and A. Vassallo, Eur. Phys. J. A **19**, 55 (2004) [nucl-th/0310041].
- [13] Q. B. Li and D. O. Riska, Phys. Rev. C **74**, 015202 (2006) [arXiv:nucl-th/0605076].
- [14] D. Y. Chen and Y. B. Dong, Commun. Theor. Phys. **50**, 142 (2008).
- [15] B. Golli, S. Sirca and M. Fiolhais, Eur. Phys. J. A **42**, 185 (2009) [arXiv:0906.2066 [nucl-th]].
- [16] I. T. Obukhovskiy, A. Faessler, D. K. Fedorov, T. Gutsche and V. E. Lyubovitskij, Phys. Rev. D **84**, 014004 (2011) [arXiv:1104.0957 [hep-ph]]; I. T. Obukhovskiy, A. Faessler, T. Gutsche and V. E. Lyubovitskij, Phys. Rev. D **89**, 014032 (2014) [arXiv:1306.3864 [hep-ph]].
- [17] V. D. Burkert and T. S. H. Lee, Int. J. Mod. Phys. E **13**, 1035 (2004) [nucl-ex/0407020].
- [18] B. Julia-Diaz, H. Kamano, T. S. H. Lee, A. Matsuyama, T. Sato and N. Suzuki, Phys. Rev. C **80**, 025207 (2009). [arXiv:0904.1918 [nucl-th]].
- [19] N. Suzuki, B. Julia-Diaz, H. Kamano, T.-S. H. Lee, A. Matsuyama and T. Sato, Phys. Rev. Lett. **104**, 042302 (2010) [arXiv:0909.1356 [nucl-th]].
- [20] J. Gegelia, U. G. Meißner and D. L. Yao, Phys. Lett. B **760**, 736 (2016) [arXiv:1606.04873 [hep-ph]].
- [21] S. Capstick and W. Roberts, Prog. Part. Nucl. Phys. **45**, S241 (2000) [nucl-th/0008028].
- [22] T. Bauer, S. Scherer and L. Tiator, Phys. Rev. C **90**, 015201 (2014) [arXiv:1402.0741 [nucl-th]].
- [23] K. L. Wang, L. Y. Xiao and X. H. Zhong, arXiv:1702.04604 [nucl-th].
- [24] D. S. Roberts, W. Kamleh and D. B. Leinweber, Phys. Rev. D **89**, 074501 (2014) [arXiv:1311.6626 [hep-lat]].
- [25] C. F. Perdrisat, V. Punjabi and M. Vanderhaeghen, Prog. Part. Nucl. Phys. **59**, 694 (2007) [hep-ph/0612014].
- [26] F. Gross, G. Ramalho and M. T. Peña, Phys. Rev. C **77**, 015202 (2008) [nucl-th/0606029].
- [27] G. Ramalho and K. Tsushima, Phys. Rev. D **84**, 054014 (2011) [arXiv:1107.1791 [hep-ph]].
- [28] G. Ramalho, K. Tsushima and A. W. Thomas, J. Phys. G **40**, 015102 (2013) [arXiv:1206.2207 [hep-ph]].
- [29] G. F. de Teramond and S. J. Brodsky, Phys. Rev. Lett. **102**, 081601 (2009) [arXiv:0809.4899 [hep-ph]].
- [30] S. J. Brodsky, G. F. de Teramond, H. G. Dosch and J. Erlich, Phys. Rept. **584**, 1 (2015) [arXiv:1407.8131 [hep-ph]].
- [31] G. F. de Teramond and S. J. Brodsky, arXiv:1203.4025 [hep-ph]. (Hadron Physics, Ferrara, Italy 2011).
- [32] S. J. Brodsky, H. C. Pauli and S. S. Pinsky, Phys. Rept. **301**, 299 (1998) [hep-ph/9705477].
- [33] S. J. Brodsky and G. F. de Teramond, Phys. Rev. D **77**, 056007 (2008) [arXiv:0707.3859 [hep-ph]].
- [34] S. J. Brodsky and G. F. de Teramond, Phys. Rev. Lett. **96**, 201601 (2006) [hep-ph/0602252].
- [35] G. F. de Teramond, H. G. Dosch and S. J. Brodsky, Phys. Rev. D **87**, 075005 (2013) [arXiv:1301.1651 [hep-ph]].
- [36] G. F. de Teramond, H. G. Dosch and S. J. Brodsky, Phys. Rev. D **91**, 045040 (2015) [arXiv:1411.5243 [hep-ph]].
- [37] D. Chakrabarti and C. Mondal, Eur. Phys. J. C **74**, 2962 (2014) [arXiv:1402.4972 [hep-ph]].
- [38] H. Forkel, M. Beyer and T. Frederico, JHEP **0707**, 077 (2007) [arXiv:0705.1857 [hep-ph]].
- [39] H. R. Grigoryan and A. V. Radyushkin, Phys. Lett. B **650**, 421 (2007) [hep-ph/0703069].
- [40] A. Ballon-Bayona, G. Krein and C. Miller, Phys. Rev. D **91**, 065024 (2015) [arXiv:1412.7505 [hep-ph]].
- [41] A. Karch, E. Katz, D. T. Son and M. A. Stephanov, Phys. Rev. D **74**, 015005 (2006) [hep-ph/0602229].
- [42] A. Ballon-Bayona, H. Boschi-Filho, N. R. F. Braga, M. Ihl and M. A. C. Torres, Phys. Rev. D **86**, 126002 (2012) [arXiv:1209.6020 [hep-ph]].
- [43] H. R. Grigoryan, T.-S. H. Lee and H. U. Yee, Phys. Rev. D **80**, 055006 (2009) [arXiv:0904.3710 [hep-ph]].
- [44] T. Branz, T. Gutsche, V. E. Lyubovitskij, I. Schmidt and A. Vega, Phys. Rev. D **82**, 074022 (2010) [arXiv:1008.0268 [hep-ph]].
- [45] A. Vega, I. Schmidt, T. Gutsche and V. E. Lyubovitskij, Phys. Rev. D **83**, 036001 (2011) [arXiv:1010.2815 [hep-ph]].
- [46] M. Ahmady, R. Sandapen and N. Sharma, Phys. Rev. D **94**, no. 7, 074018 (2016) [arXiv:1605.07665 [hep-ph]].
- [47] S. Mamedov, B. B. Sirvanli, N. Huseynova and I. Atayev, arXiv:1609.00167 [hep-th].
- [48] D. K. Hong, M. Rho, H. U. Yee and P. Yi, Phys. Rev. D **77**, 014030 (2008) [arXiv:0710.4615 [hep-ph]].
- [49] Z. Abidin and C. E. Carlson, Phys. Rev. D **79**, 115003 (2009) [arXiv:0903.4818 [hep-ph]].
- [50] T. Gutsche, V. E. Lyubovitskij, I. Schmidt and A. Vega, Phys. Rev. D **86**, 036007 (2012) [arXiv:1204.6612 [hep-ph]].
- [51] D. Chakrabarti and C. Mondal, Eur. Phys. J. C **73**, 2671 (2013) [arXiv:1307.7995 [hep-ph]].
- [52] T. Maji and D. Chakrabarti, Phys. Rev. D **94**, 094020 (2016) [arXiv:1608.07776 [hep-ph]].
- [53] T. Liu and B. Q. Ma, Phys. Rev. D **92**, 096003 (2015) [arXiv:1510.07783 [hep-ph]].
- [54] R. S. Sufian, G. F. de Teramond, S. J. Brodsky, A. Deur

- and H. G. Dosch, Phys. Rev. D **95**, 014011 (2017) [arXiv:1609.06688 [hep-ph]].
- [55] T. Gutsche, V. E. Lyubovitskij, I. Schmidt and A. Vega, Phys. Rev. D **87**, 016017 (2013) [arXiv:1212.6252 [hep-ph]].
- [56] S. J. Brodsky, D. S. Hwang, B. Q. Ma and I. Schmidt, Nucl. Phys. B **593**, 311 (2001) [hep-th/0003082].
- [57] J. M. Maldacena, Int. J. Theor. Phys. **38**, 1113 (1999) [Adv. Theor. Math. Phys. **2**, 231 (1998)] [hep-th/9711200].
- [58] S. S. Gubser, I. R. Klebanov and A. M. Polyakov, Phys. Lett. B **428**, 105 (1998) [hep-th/9802109].
- [59] E. Witten, Adv. Theor. Math. Phys. **2**, 253 (1998) [hep-th/9802150].
- [60] E. Witten, Adv. Theor. Math. Phys. **2**, 505 (1998) [hep-th/9803131].
- [61] I. R. Klebanov and M. J. Strassler, JHEP **0008**, 052 (2000) [hep-th/0007191].
- [62] T. Sakai and S. Sugimoto, Prog. Theor. Phys. **113**, 843 (2005) [hep-th/0412141].
- [63] J. Erlich, E. Katz, D. T. Son and M. A. Stephanov, Phys. Rev. Lett. **95**, 261602 (2005) [hep-ph/0501128].
- [64] L. Da Rold and A. Pomarol, Nucl. Phys. B **721**, 79 (2005) [hep-ph/0501218].
- [65] S. D. Drell and T. M. Yan, Phys. Rev. Lett. **24**, 181 (1970).
- [66] G. B. West, Phys. Rev. Lett. **24**, 1206 (1970).
- [67] A. V. Radyushkin, Acta Phys. Polon. B **26**, 2067 (1995) [hep-ph/9511272].
- [68] D. K. Hong, M. Rho, H. U. Yee and P. Yi, Phys. Rev. D **76**, 061901 (2007) [hep-th/0701276 [HEP-TH]].
- [69] T. Gutsche, V. E. Lyubovitskij, I. Schmidt and A. Vega, Phys. Rev. D **85**, 076003 (2012) [arXiv:1108.0346 [hep-ph]].
- [70] M. Henningson and K. Sfetsos, Phys. Lett. B **431**, 63 (1998) [hep-th/9803251].
- [71] W. Mueck and K. S. Viswanathan, Phys. Rev. D **58**, 106006 (1998) [hep-th/9805145].
- [72] M. Henneaux, [hep-th/9902137].
- [73] J. Polchinski and M. J. Strassler, Phys. Rev. Lett. **88**, 031601 (2002) [hep-th/0109174].
- [74] D. Melnikov and G. Ramalho, in preparation.
- [75] H. R. Grigoryan and A. V. Radyushkin, Phys. Rev. D **76**, 095007 (2007) [arXiv:0706.1543 [hep-ph]].
- [76] C. E. Carlson and F. Gross, Phys. Rev. D **36**, 2060 (1987); C. E. Carlson and N. C. Mukhopadhyay, Phys. Rev. Lett. **81**, 2646 (1998) [hep-ph/9804356].
- [77] M. J. Strassler, hep-th/0505153.
- [78] M. Krasnitz, JHEP **0212**, 048 (2002) [hep-th/0209163].
- [79] A. Dymarsky, D. Melnikov and A. Solovoy, JHEP **0905**, 105 (2009) [arXiv:0810.5666 [hep-th]].
- [80] I. Gordeli and D. Melnikov, arXiv:1311.6537 [hep-ph].
- [81] M. Berg, M. Haack and W. Mueck, Nucl. Phys. B **736**, 82 (2006) [hep-th/0507285].
- [82] I. Gordeli and D. Melnikov, JHEP **1108**, 082 (2011) [arXiv:0912.5517 [hep-th]].
- [83] I. Gordeli, *Singlet Glueballs In Klebanov-Strassler Theory*, PhD thesis; A. Dymarsky and D. Melnikov, unpublished.
- [84] S. J. Brodsky and S. D. Drell, Phys. Rev. D **22**, 2236 (1980).
- [85] J. Arrington, W. Melnitchouk and J. A. Tjon, Phys. Rev. C **76**, 035205 (2007) [arXiv:0707.1861 [nucl-ex]]. A. J. R. Puckett *et al.*, Phys. Rev. Lett. **104**, 242301 (2010) [arXiv:1005.3419 [nucl-ex]].
- [86] M. Ostrick *et al.*, Phys. Rev. Lett. **83**, 276 (1999); C. Herberg *et al.*, Eur. Phys. J. A **5**, 131 (1999); D. I. Glazier *et al.*, Eur. Phys. J. A **24**, 101 (2005) [arXiv:nucl-ex/0410026]; I. Passchier *et al.*, Phys. Rev. Lett. **82**, 4988 (1999) [arXiv:nucl-ex/9907012]; T. Eden *et al.*, Phys. Rev. C **50**, 1749 (1994); H. Zhu *et al.* [E93026 Collaboration], Phys. Rev. Lett. **87**, 081801 (2001) [arXiv:nucl-ex/0105001]; R. Madey *et al.* [E93-038 Collaboration], Phys. Rev. Lett. **91**, 122002 (2003) [arXiv:nucl-ex/0308007]; G. Warren *et al.* [Jefferson Lab E93-026 Collaboration], Phys. Rev. Lett. **92**, 042301 (2004) [arXiv:nucl-ex/0308021]; S. Riordan *et al.*, Phys. Rev. Lett. **105**, 262302 (2010) arXiv:1008.1738 [nucl-ex]; R. Schiavilla and I. Sick, Phys. Rev. C **64**, 041002 (2001) [arXiv:nucl-ex/0107004].
- [87] P. E. Bosted, Phys. Rev. C **51**, 409 (1995); G. Kubon *et al.*, Phys. Lett. B **524**, 26 (2002) [arXiv:nucl-ex/0107016]; H. Anklin *et al.*, Phys. Lett. B **428**, 248 (1998); H. Anklin *et al.*, Phys. Lett. B **336**, 313 (1994); J. Lachniet *et al.* [CLAS Collaboration], Phys. Rev. Lett. **102**, 192001 (2009) [arXiv:0811.1716 [nucl-ex]].
- [88] I. G. Aznauryan *et al.* [CLAS Collaboration], Phys. Rev. C **80**, 055203 (2009) [arXiv:0909.2349 [nucl-ex]].
- [89] V. I. Mokeev *et al.* [CLAS Collaboration], Phys. Rev. C **86**, 035203 (2012) [arXiv:1205.3948 [nucl-ex]]; V. I. Mokeev *et al.*, Phys. Rev. C **93**, 025206 (2016) [arXiv:1509.05460 [nucl-ex]].
- [90] V. I. Mokeev, https://userweb.jlab.org/~mokeev/resonance_electrocouplings/
- [91] G. Ramalho, in preparation.
- [92] G. Ramalho and M. T. Peña, Phys. Rev. D **80**, 013008 (2009) [arXiv:0901.4310 [hep-ph]].
- [93] G. Ramalho and K. Tsushima, Phys. Rev. D **82**, 073007 (2010) [arXiv:1008.3822 [hep-ph]].
- [94] G. Ramalho, D. Jido and K. Tsushima, Phys. Rev. D **85**, 093014 (2012) [arXiv:1202.2299 [hep-ph]].
- [95] G. Ramalho and K. Tsushima, Phys. Rev. D **88**, 053002 (2013) [arXiv:1307.6840 [hep-ph]]; G. Ramalho and K. Tsushima, Phys. Rev. D **87**, 093011 (2013) [arXiv:1302.6889 [hep-ph]].
- [96] G. Ramalho and M. T. Peña, Phys. Rev. D **89**, 094016 (2014) [arXiv:1309.0730 [hep-ph]].
- [97] G. Ramalho, Phys. Rev. D **90**, 033010 (2014) [arXiv:1407.0649 [hep-ph]].
- [98] G. Ramalho, M. T. Peña, J. Weil, H. van Hees and U. Mosel, Phys. Rev. D **93**, 033004 (2016) [arXiv:1512.03764 [hep-ph]].
- [99] G. Ramalho, Phys. Rev. D **94**, 114001 (2016) [arXiv:1606.03042 [hep-ph]].
- [100] G. Ramalho, arXiv:1612.09555 [hep-ph].
- [101] O. Krehl, C. Hanhart, S. Krewald and J. Speth, Phys. Rev. C **62**, 025207 (2000) [nucl-th/9911080].
- [102] M. Doring, C. Hanhart, F. Huang, S. Krewald and U.-G. Meissner, Nucl. Phys. A **829**, 170 (2009) [arXiv:0903.4337 [nucl-th]].
- [103] Z. W. Liu, W. Kamleh, D. B. Leinweber, F. M. Stokes, A. W. Thomas and J. J. Wu, arXiv:1607.04536 [nucl-th].
- [104] C. B. Lang, L. Leskovec, M. Padmanath and S. Prelovsek, Phys. Rev. D **95**, 014510 (2017) [arXiv:1610.01422 [hep-lat]].